ACADEMIC PRESS

Available online at www.sciencedirect.com

SCIENCE DIRECT®

Developmental Biology 261 (2003) 39–54

DEVELOPMENTAL BIOLOGY

www.elsevier.com/locate/ydbio

FGF-10 plays an essential role in the growth of the fetal prostate

Annemarie A. Donjacour,[a,*] Axel A. Thomson,[b] and Gerald R. Cunha[a,c]

[a] *Department of Anatomy, University of California at San Francisco, 513 Parnassus Avenue, San Francisco, CA 94143, USA*
[b] *MRC Human Reproductive Sciences Unit, University of Edinburgh Chancellor's Building, 49 Little France Crescent, Edinburgh EH16 4SB, UK*
[c] *Department of Urology, University of California at San Francisco, 513 Parnassus Avenue, San Francisco, CA 94143, USA*

Received for publication 27 August 2002, revised 11 April 2003, accepted 21 April 2003

Abstract

Induction and branching morphogenesis of the prostate are dependent on androgens, which act via the mesenchyme to induce prostatic epithelial development. One mechanism by which the mesenchyme may regulate the epithelium is through secreted growth factors such as FGF-10. We have examined the male reproductive tract of FGF-$10^{-/-}$ mice, and at birth, most of the male secondary sex organs were absent or atrophic, including the prostate, seminal vesicle, bulbourethral gland, and caudal ductus deferens. Rudimentary prostatic buds were occasionally observed in the prostatic anlagen, the urogenital sinus (UGS) of FGF-$10^{-/-}$ mice. FGF-$10^{-/-}$ testes produced sufficient androgens to induce prostatic development in control UGS organ cultures. Prostatic rudiments from FGF-$10^{-/-}$ mice transplanted into intact male hosts grew very little, but showed some signs of prostatic differentiation. In cultures of UGS, the FGF-10 null phenotype was partially reversed by the addition of FGF-10 and testosterone, resulting in the formation of prostatic buds. FGF-10 alone did not stimulate prostatic bud formation in control or FGF-$10^{-/-}$ UGS. Thus, FGF-10 appears to act as a growth factor which is required for development of the prostate and several other accessory sex organs.

Introduction

The prostate is a branched ductal gland whose mesenchymal–epithelial interactions are under the control of systemic androgens (Cunha et al., 1987). In embryonic and neonatal development, androgens act indirectly via mesenchymal androgen receptors to regulate epithelial proliferation, budding, ductal branching, and apoptosis (Cunha et al., 1987; Kurita et al., 2001). The paracrine mediators of androgen action have not been conclusively identified, but FGFs are promising candidates (Lu et al., 1999; Thomson, 2001; Thomson and Cunha, 1999).

The fibroblast growth factors (FGF) constitute a family of heparin-binding growth signals that play key roles in organogenesis (Hogan, 1999; Szebenyi and Fallon, 1999). There are at least 22 FGF ligands (reviewed in Szebenyi and Fallon, 1999). These ligands each interact with a subset of FGF receptors. There are 4 genes coding for FGF receptors, each of which have multiple splice variants (reviewed in McKeehan et al., 1998). The FGF receptors are dimeric tyrosine kinase receptors that signal through the ras/raf/MAPK pathway as well as via PLCγ/DAG and Ca^{2+} release (Szebenyi and Fallon, 1999). The cellular effects of FGFs include survival, proliferation, chemotaxis, differentiation, and regulation of other growth factors and nuclear factors (reviewed in Szebenyi and Fallon, 1999). Some FGF family members are expressed at high levels in male reproductive tract organs during embryonic and neonatal stages and subsequently decline (Thomson and Cunha, 1999; Thomson et al., 1997).

During organogenesis, several FGF family members play a significant role in mesenchymal–epithelial interactions. Fibroblast growth factor-4, FGF-7 (also known as KGF), and FGF-10 are expressed in the mesenchyme, while their receptors are predominantly found on adjacent epithelial cells (Finch et al., 1995; Mason et al., 1994; Orr-Urtreger et al., 1993). In limb formation, FGF-10 is expressed in a restricted area of the lateral plate mesoderm. It induces the differentiation of the apical ectodermal ridge from the surface ectoderm and promotes limb outgrowth (Martin, 2001).

Mechanisms of branching morphogenesis often involve

* Corresponding author. Fax: +1-415-502-2270.
E-mail address: adonj@itsa.ucsf.edu (A.A. Donjacour).

0012-1606/03/$ – see front matter © 2003 Elsevier Inc. All rights reserved.
doi:10.1016/S0012-1606(03)00250-1

FGFs. Lung development in both mice and *Drosophila* requires FGF-10 (in *Drosophila* branchless), which appears to be a key growth factor and chemotaxic agent (Min et al., 1998; Park et al., 1998; Peters et al., 1994; Sekine et al., 1999; Sutherland et al., 1996). FGF-10 is also involved during development in other organs that undergo branching morphogenesis, such as the lacrimal gland (Govindarajan et al., 2000) and pancreas (Bhushan et al., 2001).

In the developing prostate and seminal vesicle, messenger RNAs for FGF-7 and FGF-10 are localized in the mesenchyme (Finch et al., 1995; Thomson and Cunha, 1999). The receptor for FGF-7 and -10 are found in the epithelium of the urogenital sinus and Wolffian duct (Finch et al., 1995). Both FGF-7 and FGF-10 can substitute for testosterone in organ cultures of neonatal rat prostate, supporting extensive epithelial growth and ductal branching morphogenesis (Sugimura et al., 1996; Thomson and Cunha, 1999).

Redundancy of FGF-7 signaling appears to operate during development. FGF-$7^{-/-}$ mice exhibit no obvious abnormalities aside from a rough coat (Guo et al., 1996). Even the lungs, whose branching morphogenesis is affected by FGF-7 overexpression (Simonet et al., 1995) and FGFR2b inhibition (Peters et al., 1994), developed normally in FGF-$7^{-/-}$ mice (Guo et al., 1996). No prostatic phenotype or problems with fertility have been noted in these mice (Guo et al., 1996). FGF-$10^{-/-}$ mice have been created (Min et al., 1998; Sekine et al., 1999). These mice die at birth and lack lungs and limbs; they also have abnormalities in skin differentiation (Suzuki et al., 2000). The phenotype of the male reproductive organs of FGF-$10^{-/-}$ mice has not been described. In this study, the reproductive tracts of FGF-$10^{-/-}$ mice have been examined.

Materials and methods

Animals

FGF-$10^{+/-}$ breeding pairs were generously provided by W. Scott Simonet (Amgen, Thousand Oaks, CA). Mice were mated and FGF-$10^{-/-}$ embryos were recognized by their lack of limbs (Min et al., 1998; Sekine et al., 1999). Heterozygous mice were identified by PCR of genomic tail DNA. The primers were: wild-type 5′-CAT TGT GCC TCA GCC TTT CCC, shared 5′-ACT CTT TGG CCT CTA TCT AG, null 5′-CAC CAA AGA ACG GAG CCG GTT G. For timed pregnant matings, the plug date is day zero. CD1 Nu/Nu (nude) male mouse hosts for grafting were obtained from Charles River (Wilmington, MA).

Dissection and photography

Organ rudiments were dissected from fetuses and photographed with a Dage MTI DC330 digital camera (Michigan City, IN) mounted on a compound or dissecting microscope. Testes from embryos at 15-16 days postconception (dpc, also known as E15–E16) and urogenital sinuses (UGSs) that had been cultured were fixed and photographed to estimate organ size, as these organs were too small for wet weight measurement. Organ area was calculated by using the public domain program, NIH Image (developed at U.S. NIH and available on the internet at http://rsb.info.nih.gov/nih-image/). Adobe Photoshop (Mountain View, CA) software was used to acquire and process images. Statistical differences between two groups were calculated by using the Student's *t* test, and differences among several groups were calculated by using an analysis of variance followed by a Fisher's PLSD test.

Tissue recombination and grafting

To compare the androgenic ability of control and FGF-$10^{-/-}$ fetal testes, these rudiments were grafted under the kidney capsule of castrated adult nude mouse hosts. Mice were anesthetized with avertin (Jones and Krohn, 1960) and castrated via the scrotal route. Following at least 2 weeks to allow for full prostatic regression, fetal testes were grafted (2 per host mouse) under the kidney capsule (Cunha and Donjacour, 1987). One month after grafting, the hosts were euthanized, and their prostatic lobes and seminal vesicles were weighed and examined histologically for evidence of androgen action. To examine the developmental potential of the male accessory sex organs from FGF-10 null mice, ages 15 dpc to birth, embryonic rudiments, i.e., the UGS, Wolffian duct (WD), and caudal pelvic urethra (precursor region for the bulbourethral gland), were grafted under the renal capsules of adult, intact male nude mice (Cunha and Donjacour, 1987). This allows organ growth and development in the presence of adult levels of testosterone over an extended time. Some UGSs were harvested 2 weeks after grafting to assess proliferation and apoptosis, while the rudiments were actively growing. Grafted organ rudiments were also recovered following 1 month of grafting to evaluate differentiation and organ wet weight.

Tissue recombinants were made by using urogenital sinus mesenchyme (UGM) and urogenital sinus epithelium (UGE) or embryonic bladder epithelium (BLE) from control (wild-type or heterozygous) and FGF-10 null mice as previously described (Cunha and Donjacour, 1987). UGM and UGE from both male mice (15-16.5 dpc) and female mice (15-19 dpc) were used. Tissue recombinants were harvested 1 month after grafting, weighed, and examined histologically.

Histology

Fetal organs and grafts were fixed by immersion for 1-2 h at room temperature in neutral buffered formalin. For paraffin sections, tissues were dehydrated, cleared in Histoclear (National Diagnostics, Atlanta, GA), and embedded. Tissues were cut 6 μm in thickness. For plastic sections,

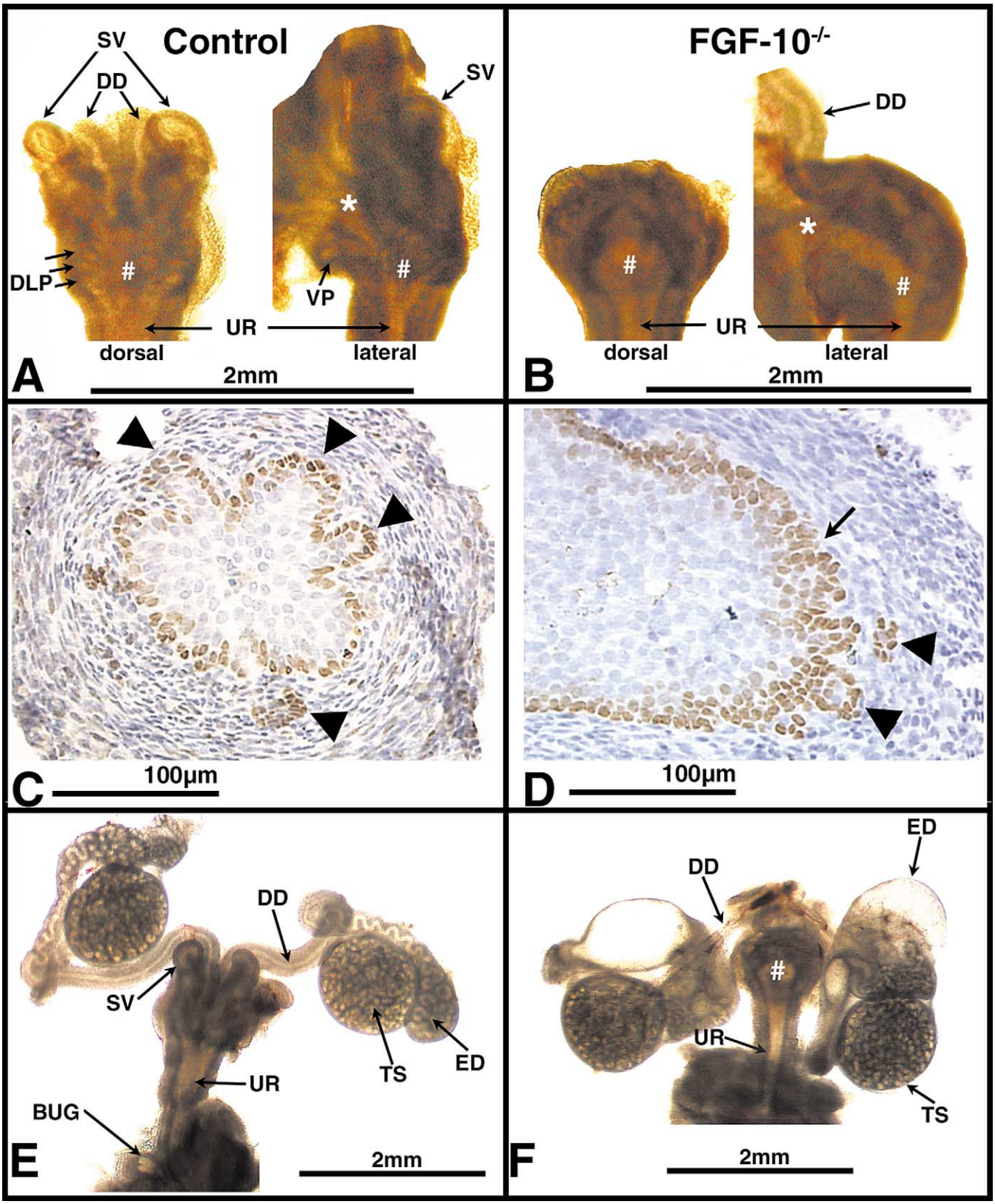

Fig. 1. Whole-mount (A, B, E, F) and histology (C, D) of male reproductive tracts from control (A, C, E) and FGF-$10^{-/-}$ (B, D, F) embryos. (A) At 19 dpc in control males, both the dorsal (DLP) and ventral (VP) prostatic buds were visible budding from the urogenital sinus (#), distal to the bladder neck (*), and proximal to the urethra (UR). The seminal vesicles (SV) were visible to either side of the ductus deferens (DD). (B) In FGF-$10^{-/-}$ males, the urogenital sinus (#) and urethra (UR) were visible distal to the bladder neck (*), but prostatic buds were not discernable. In some embryos, the ductus deferens (DD) remained. (C) The control UGS at 18.5 dpc stained with anti-p63 anti-body (brown), which stains basal epithelial cells, and hematoxylin. Prostatic buds were

formalin-fixed tissues were dehydrated to 95% ethanol and embedded in JB-4 plastic (Polysciences, Warrington, PA), sectioned at 3 μm, and stained with methylene blue.

Immunocytochemistry

Prostatic and seminal vesicle secretory proteins were detected in sections by using rabbit polyclonal antibodies to mouse dorsolateral prostate, ventral prostate, and seminal vesicle as previously described (Donjacour et al., 1990; Higgins et al., 1989). To visualize nuclear markers, i.e., androgen receptors, Ki67, and p63, sections were deparaffinized and rehydrated; antigens were unmasked by boiling sections in citrate buffer, pH 6, (Antigen Unmasking solution; Vector Laboratories Burlingame, CA) for 30 min in a microwave oven. Blocking solution (Superblock; Pierce, Rockford, IL) was applied to sections followed by the primary antibody (anti-androgen receptor,1:50; Affinity Bioreagents, Golden, CO; anti-p63 antiserum, 1:100; Santa Cruz Biotechnology, Santa Cruz, CA; or anti-Ki67, 1:200; Novocast Laboratories, Newcastle, UK). Antibody binding was detected by using secondary anti-rabbit or anti-mouse IgG antibodies (Amersham, Piscataway, NJ) and the ABC peroxidase method (Vector Laboratories).

To assess proliferation, random paraffin sections of UGS grown for 2 weeks or UGSs dissected directly from 17-19 dpc male embryos were subjected to antigen retrieval and were stained immunocytochemically with anti-Ki 67 (Gallee et al., 1989). A minimum of 2500 cells (5 separate fields) from 3-10 organs or grafts were counted to measure Ki67 labeling index.

Apoptosis was detected with the terminal transferase reaction by using the ApopTag peroxidase kit (Intergen Co., Purchase, NY).

Organ culture

UGSs from male and female fetuses, ages 15-18 dpc, were cultured on Millicell CM filters (Millipore Corp, Bedford, MA) floating on 1 ml of medium [DMEM H16:Ham's F12 (1:1/vol.) supplemented with 10 g/ml insulin, 5 μg/ml transferrin, 100U/ml penicillin,100 μg/ml streptomycin, and 25 μg/ml fungizone (UCSF cell culture facility)] (Foster et al., 1999). Testosterone (10^{-8} M; Steraloids, Wilton NH) and/or human FGF-10 (100 or 200 ng/ml; BioVision Inc., Mt. View, CA) were added. Male UGSs from 16-day-old fetuses were cocultured with testes of the same age from either control or FGF-10 null fetuses. One or two testes and one UGS were placed in contact on a filter and floated on serum-free medium lacking testosterone. Medium was changed every 2 days for 4 days.

Results

Offspring from FGF-$10^{+/-}$ matings were examined by gross dissection from the age of 15 dpc until birth. At all ages studied, FGF-$10^{+/+}$ and FGF-$10^{+/-}$ animals were not different from each other as judged by body weight, crown-rump length, and organ weights. These observations were in agreement with Min et al. (1998). For the purposes of this study, FGF-$10^{+/+}$ and FGF-$10^{+/-}$ animals were grouped together and were referred to as "controls." As previously described, FGF-$10^{-/-}$ mice died at birth and were identifiable embryonically by an absence of limbs (Min et al., 1998; Sekine et al., 1999).

In FGF-$10^{-/-}$ mice, the prostate was not visible at the end of gestation in whole-mount preparations, whereas prostatic buds were observed in control mice (Fig. 1A and B). In histologic sections of control urogenital sinuses (UGSs) and neonatal prostates, the basal lamina and the bud distribution were difficult to see with routine hematoxylin and eosin staining. Late gestation UGSs were therefore stained with other markers to delineate prostatic buds. These markers included p63, a nuclear protein found in basal cells of many organs including the prostate (Signoretti et al., 2000), and androgen receptors. In control UGSs, numerous prostatic buds were visible (Fig. 1C). In FGF$^{-/-}$ UGSs, however, the epithelial contours were generally smooth. Occasionally, buds or indentations of the basal lamina were observed (Fig. 1D).

The seminal vesicles (SV) and bulbourethral glands were also absent in FGF-$10^{-/-}$ embryos (Fig. 1E and F). The caudal portion of the WD, 25% of the length of the WD nearest the UGS, was present in FGF-$10^{-/-}$ embryos 15 dpc and younger, but by 18 dpc, it was absent in a majority of the FGF-$10^{-/-}$ males. When present, it was much thinner than in controls. Testes and epididymides were always present; in animals in which the caudal WD was absent, the epididymis was cystic (Fig. 1F). The absence or atrophy of the male secondary sex organs except the epididymis raised the possibility that testicular function was compromised in the FGF-$10^{-/-}$ mutants.

Testicular size in FGF-$10^{-/-}$ males, as estimated by area in photographs of testes, was not different from that of controls (data not shown). The histology of the testes from FGF-10 mice appeared to be normal (Fig. 2A and B). Cystic epididymides in FGF-$10^{-/-}$ mice maintained a columnar

clearly visible (arrowheads). (D) The FGF-$10^{-/-}$ UGS, stained as in (C), had a small number of buds (arrowheads) and more subtle indentations of the basal lamina (arrow). (E) A view of the whole reproductive tract of a control male at 17.5 dpc, dorsal view, revealed the testes (TS), epididymis (ED), SV, and DD cranial to the urogenital sinus. One of the paired bulbourethral gland (BUG) is indicated at the caudal-most end of the pelvic urethra. (F) The FGF-$10^{-/-}$ male reproductive tract had testes of normal size, but the ductus deferens was highly attenuated and the epididymides were cystic. The seminal vesicles and bulbourethral glands were absent.

epithelium in the corpus, and the expanded lumen often contained cellular debris. Numerous apoptotic bodies were observed in both the epithelium and stroma of FGF-10$^{-/-}$ epididymides (Fig. 2C and D).

As fetal tissue and blood were too limited, functional assays of androgen production were used. Fetal testes were grafted under the renal capsules of castrated male nude mouse hosts. One month after grafting control and FGF-10 $^{-/-}$ testes were equally effective in stimulating growth of the host ventral prostate (VP), increasing the wet weight of the VP 4-fold (control, $n = 2$) and 3.8-fold (FGF-10$^{-/-}$, $n = 2$) compared with that of castrate hosts without testicular grafts. However, in hosts grafted with FGF-10$^{-/-}$ testes, the dorsolateral prostate (DLP) and coagulating gland (CG) were only 2.5-fold larger than those of the castrates, while DLP and CG from hosts grafted with control testes were 3.6- and 4.5-fold larger. FGF-10$^{-/-}$ testes appeared to have appreciable capacity to produce testosterone, though possibly less than that of controls.

Testicular function was also assessed by an in vitro method. Testes were cocultured with the prostatic precursor, the UGS, and the SV to determine whether FGF-10$^{-/-}$ testes could support development of control male secondary sex organs. The reciprocal experiment was also performed in which control testes were cocultured with FGF-10$^{-/-}$ UGSs. Tissues were taken at 16 dpc, a time at which control prostatic buds had not yet emerged from the urogenital sinus epithelium, and the seminal vesicle epithelium was unfolded. After 4 days in culture, prostatic buds were visible in control UGSs cocultured with control testes, and the SV epithelium developed infoldings (Fig. 3A). Prostatic buds and SV epithelial infolding were also clearly present in control UGSs and SVs cocultured with FGF-10$^{-/-}$ testes (Fig. 3B). Conversely, buds did not form in FGF-10$^{-/-}$ UGSs, even when they were cocultured with control testes (Fig. 3C and D). FGF-10$^{-/-}$ testes supported in vitro growth of control UGSs, but FGF-10$^{-/-}$ UGSs were unable to respond to control testes.

To provide a more rigorous test of the ability of the UGS from FGF-10$^{-/-}$ mice to form prostate, FGF-10$^{-/-}$ prostatic rudiments were grafted under the renal capsule of intact adult nude mice. In this environment, the UGS was exposed to adult levels of androgens for a period of 1 month. Under these circumstances, control UGSs of both males and females, at all embryonic ages, give rise to prostatic tissue (Cunha, 1975; Cunha et al., 1980) (Fig. 4A and C). Urogenital sinuses from the FGF-10$^{-/-}$ mice exhibited some growth, but the wet weight of the grafts was significantly less than the controls (Fig. 5). Grafts of FGF-10 $^{-/-}$ urogenital sinuses did not develop branching ducts, but after 1 month, more closely resembled the original UGS at the time of grafting. The host circulation or kidney parenchyma did not appear to contribute to the growth of the grafted FGF-10$^{-/-}$ UGS. The epithelium was mostly stratified (Fig. 4B and D). In some places, however, there were out-pocketings of simple columnar or cuboidal epithelium. These out-pocketings sometimes contained material that stained with anti-serum to mouse DLP secretory proteins (anti-mDLP). Intracellular staining was also observed (Fig. 4B). Control UGS grafts developed complex branched ductal networks. Extensive luminal and some intracellular staining with anti-mDLP were seen in control UGS grafts (Fig. 4A). The majority of epithelial and mesenchymal cells in control and FGF-10$^{-/-}$ UGS grafts contained androgen receptors, as judged by immunocytochemical staining (Fig. 4C and D).

Proliferation was measured by counting Ki67-labeled cells in UGSs grafts, 16.5-17.5 dpc at the start, grown for 2 weeks, a time at which the tissue is actively growing (Cunha et al., 1983). Mesenchymal labeling was equal in the grafts of control and FGF-10$^{-/-}$ UGS (Fig. 6A). However, the epithelium in control grafts had a significantly higher labeling index than that of FGF-10$^{-/-}$ grafts (Fig. 6B). In urogenital sinuses taken from embryos in the midst of the budding stage of prostatic growth in vivo (~18.5 dpc), the UGM and UGE from control and FGF-10$^{-/-}$ mice labeled equivalently with Ki67 antibody (Fig. 6C and D). However, in the control UGS grafts, the prostatic buds had a significantly higher proliferation rate (Fig. 6C and D) than UGE from either control or FGF-10$^{-/-}$ mice. Indentations of the UGE basal lamina were associated with areas that appeared to contain more proliferating epithelial cells than other parts of the UGE in FGF-10$^{-/-}$ grafts. (Fig. 6D).

Neither apoptotic bodies nor TUNEL staining was observed in the late gestation male UGSs and developing prostates of control and FGF-10$^{-/-}$ mice. Control and FGF-10$^{-/-}$ UGSs grown for 2 weeks had similarly low apoptotic rates (data not shown).

Control and FGF-10$^{-/-}$ UGSs at 15-17.5 dpc were cultured for 4 days in serum-free medium. In the absence of testosterone, buds did not form in UGSs of any genotype (data not shown). In the presence of 10^{-8} M testosterone, control UGSs formed ducts; these ducts were generally unbranched (Fig. 7A). FGF-10$^{-/-}$ UGSs did not form buds or ducts when cultured with testosterone alone (Fig 7B). FGF-10 alone (100 or 200 ng/ml) never induced budding in the absence of testosterone in either control or FGF-10$^{-/-}$ UGSs (Fig. 7C). FGF-10 alone or in combination with testosterone did not induce growth in control UGSs in culture as measured by explant area (Fig. 7D). FGF-10$^{-/-}$ UGSs cultured with testosterone plus FGF-10 grew significantly less than controls; however, these FGF-10$^{-/-}$ sinuses developed prostatic buds, partially reversing the FGF-10 null phenotype (Fig. 7F). Control UGSs cultured with testosterone and FGF-10 seemed to have wider ducts and have somewhat more branching per duct than those culture with testosterone alone (T: 0.05 ± .02 branch-points/duct, $n = 13$; T+FGF-10: 0.10 ± .02, $n = 14$, $P = 0.09$) (Fig. 7E).

In FGF-10$^{-/-}$ fetuses older than 16 dpc, the caudal portion of the WD, near the UGS, was usually absent or extremely thin (Fig. 1F). However, in some male FGF-10$^{-/-}$ fetuses, the caudal WD was still present. When this

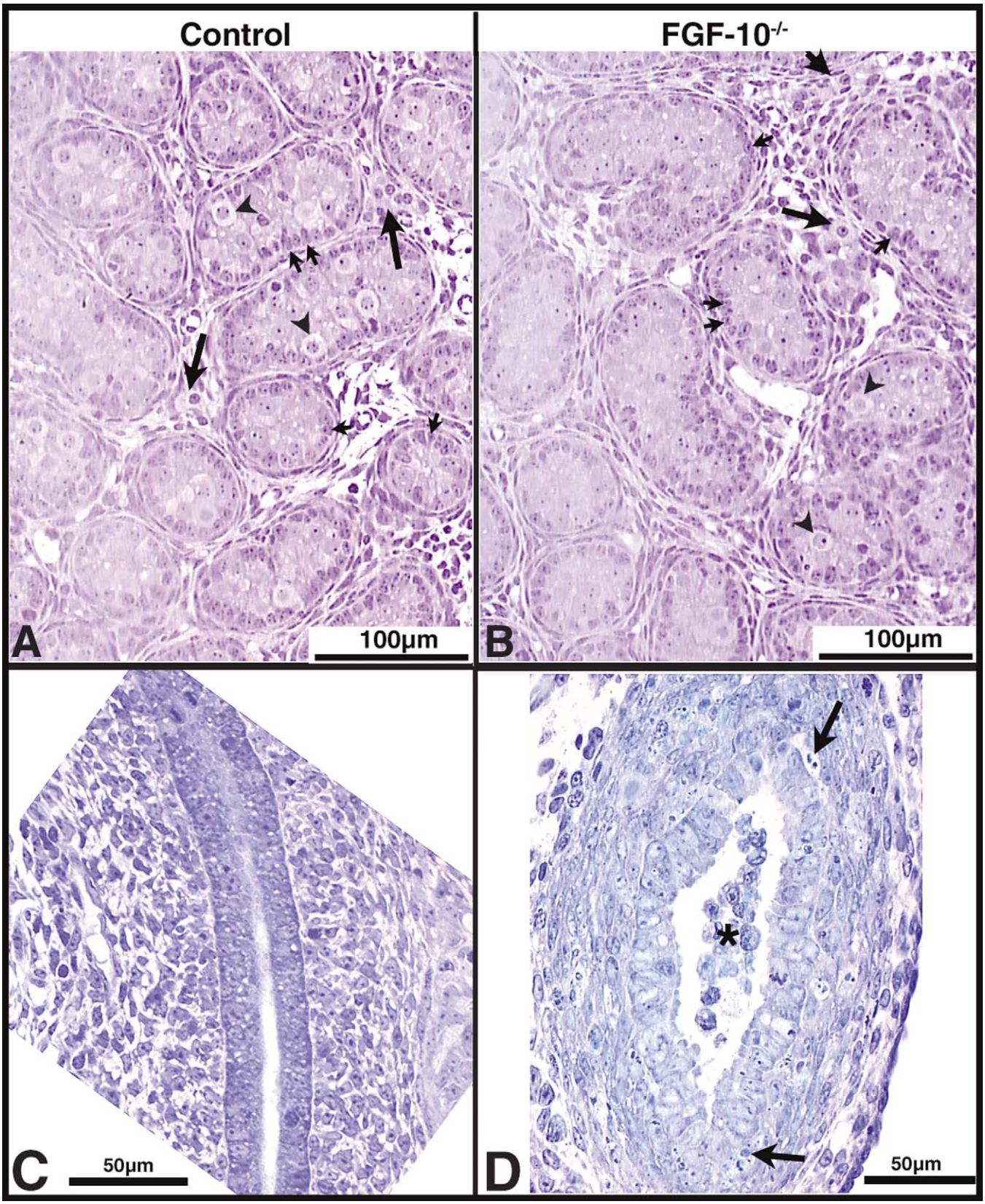

Fig. 2. Testes and epididymides from control (A, C) and FGF-$10^{-/-}$ (B, D) males. JB-4 sections stained with methylene blue. (A) Control testes at 18.5 dpc had abundant Sertoli cells (small arrows) lining the seminiferous tubules, scattered germ cells (arrowheads), and prominent fetal Leydig cells (large arrows). (B) FGF-$10^{-/-}$ testes at 18.5dpc were very similar to the controls. (C) Body (corpus) of the epididymis from a control male at 16 dpc. (D) Body (corpus) of the epididymis from a FGF-$10^{-/-}$ male at 16 dpc. The distal part of the Wolffian duct from this fetus had degenerated causing the ductus deferens to become cystic. Note the numerous apoptotic bodies (arrows) and the dead cells in the lumen (*).

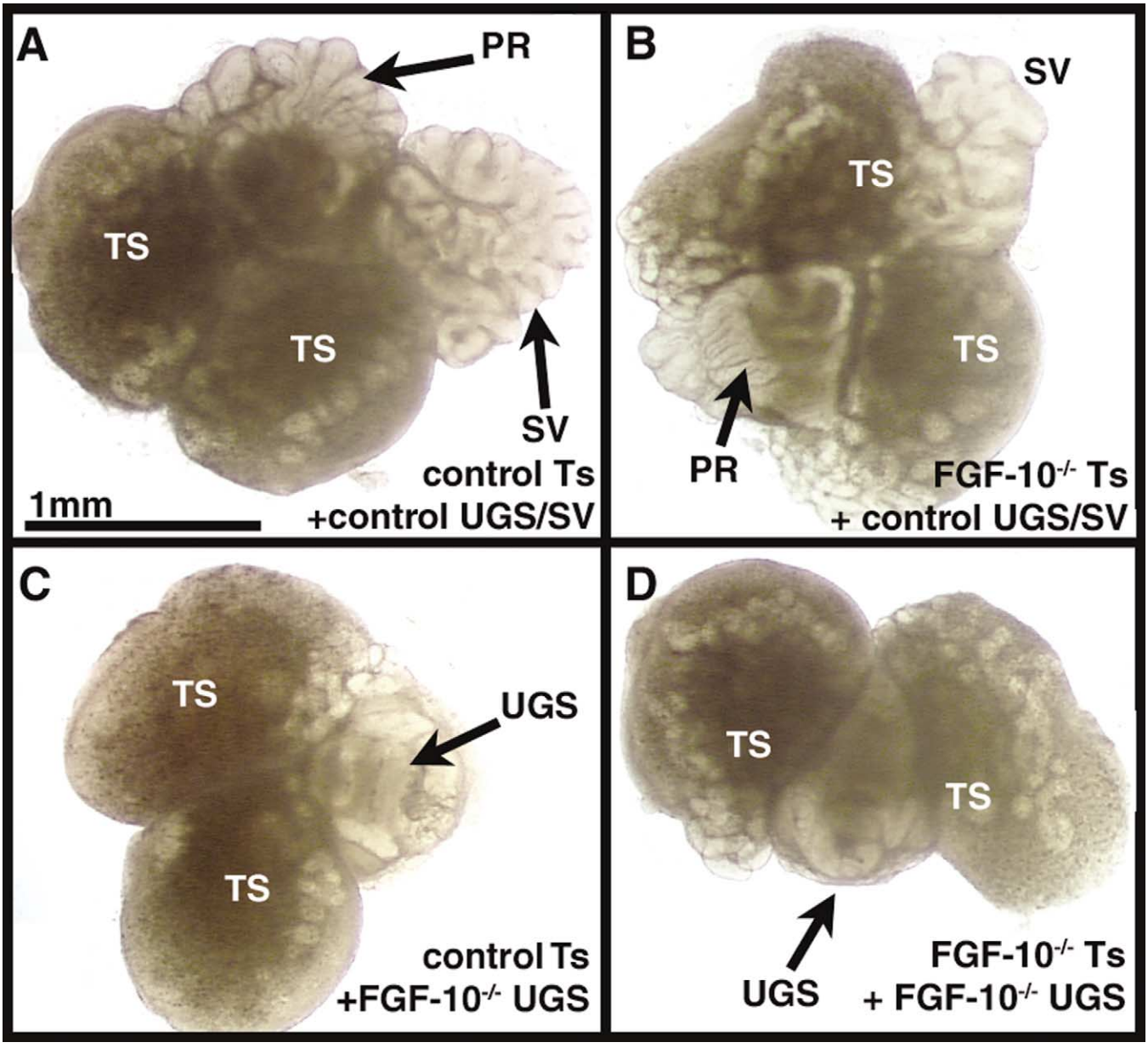

Fig. 3. Coculture of testes (TS) and urogenital sinus (UGS) from control and FGF-$10^{-/-}$ males (16 dpc, $n = 3$ per group). (A) Control testes stimulated prostatic bud (PR) growth from control UGS and infolding of control seminal vesicle (SV) rudiments. (B) FGF-$10^{-/-}$ testes also induced prostatic bud (PR) growth from control UGS and infolding of the SV, though perhaps not to the same extent as normal testes (A). (C) Control testes did not stimulate bud outgrowth from FGF-$10^{-/-}$ UGS. (D) FGF-$10^{-/-}$ UGS cultured with FGF-$10^{-/-}$ testes showed no ductal outgrowth.

area was grown under the renal capsule, the majority of grafts of FGF-$10^{-/-}$ caudal WD contained stroma alone (5/8) or tissue that resembled ductus deferens (2/8). In one of eight grafts of FGF-$10^{-/-}$ caudal WD, tissue resembling immature SV was observed; this tissue stained with antiserum to mouse seminal vesicle secretion (Fig. 8B). In contrast, grafting a comparable area of control WD yielded either ductus deferens only (1/6), seminal vesicle only (2/6), or both (3/6) (Fig. 8A). Thus, the caudal WD from the FGF-$10^{-/-}$ mice had a very limited ability to develop into SV. When the caudal urethral area from control mice was grafted, bulbourethral gland tissue developed; this did not occur when FGF-$10^{-/-}$ caudal urethral tissue was grafted. Instead, abundant stroma and a tube of stratified epithelium were observed (Fig. 8C and D). Thus, FGF-$10^{-/-}$ caudal urethra did not produce bulbourethral gland in this graft environment.

Discussion

The male secondary sex organs of FGF-$10^{-/-}$ mice were almost entirely absent at birth, with the epididymis and the cranial portion of the WD being the only remaining accessory sexual structures. The explanation for this phenotype is

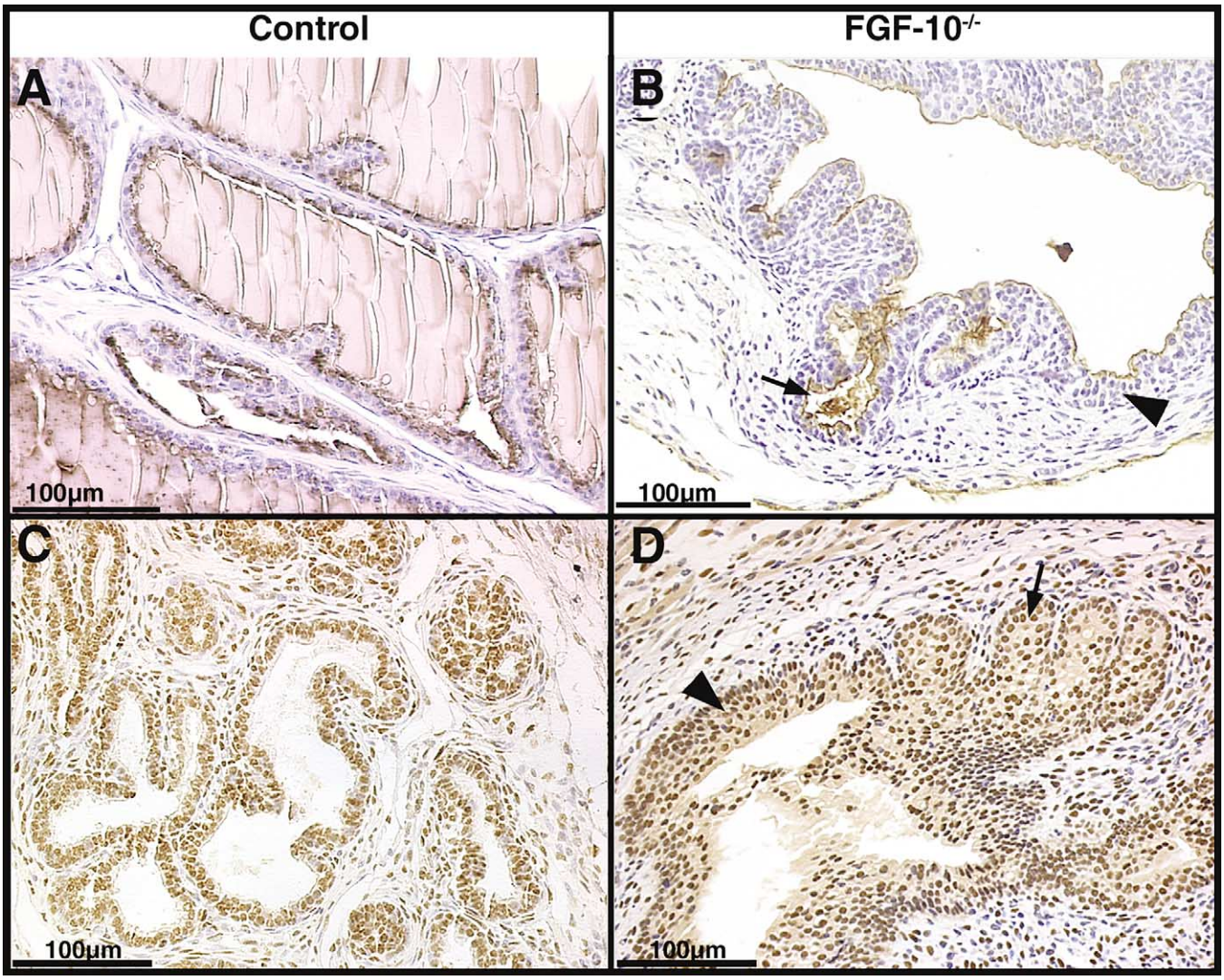

Fig. 4. Histology and immunocytochemistry of grafted UGS from control (A, C) and FGF-$10^{-/-}$ (B, D) males grown in intact hosts for 1 month. (A) Anti-mDLP-stained section of control UGS (18 dpc at grafting). (B) Anti-mDLP-stained section of FGF-$10^{-/-}$ UGS (18 dpc at grafting). A bud is indicated by an arrow, and stratified epithelium similar to UGE is indicated by an arrowhead. (C) Anti-androgen receptor-stained section of control UGS (16.5 dpc at grafting). (D) Anti-androgen receptor-stained section of FGF-$10^{-/-}$ UGS (17.5 dpc at grafting). A bud is indicated by an arrow, and stratified epithelium similar to UGE is indicated by an arrowhead.

likely to be twofold. First, testosterone levels appear to be somewhat reduced in the FGF-$10^{-/-}$ males, and testosterone is required for development of all male secondary sex organs. Second, FGF-10 is required within these organs themselves for their development.

FGF-$10^{-/-}$ mice lack a pituitary gland (Ohuchi et al., 2000), the source of luteinizing hormone (LH). In fetal life, however, LH does not appear to play a role in stimulating testosterone production as it does in adults (Jost, 1971; O'Shaughnessy et al., 1998). When FGF-$10^{-/-}$ testes were grafted under the renal capsule of castrated males, prostatic wet weights were stimulated significantly although less than by control testes. Also, FGF-$10^{-/-}$ testes stimulated control UGS and SV development in coculture. Thus, the fetal FGF-$10^{-/-}$ testes produce androgens at levels sufficient to induce and promote prostatic and SV development.

The absence of the lower WD in FGF-$10^{-/-}$ embryos is difficult to interpret with regard to the relative contributions of testosterone and FGF-10. In FGF-$10^{-/-}$ embryos, the entire WD was originally present in all of the embryos 15 dpc and younger. The epididymis and cranial ductus deferens persisted through gestation. Thus, the absence of the caudal WD was due to regression of a preexisting structure. Complete WD retention requires testosterone at a critical threshold level. When testosterone levels are reduced, the WD are known to be only partially retained (Jost, 1971). Therefore, the absence of the caudal portion of the WD in FGF-$10^{-/-}$ embryos could be due to suboptimal testosterone production by the FGF-$10^{-/-}$ testes.

Alternatively, the absence of the caudal WD in FGF-$10^{-/-}$ embryos may highlight a key role of FGF-10 as a mediator of androgen action in WD maintenance. Only one

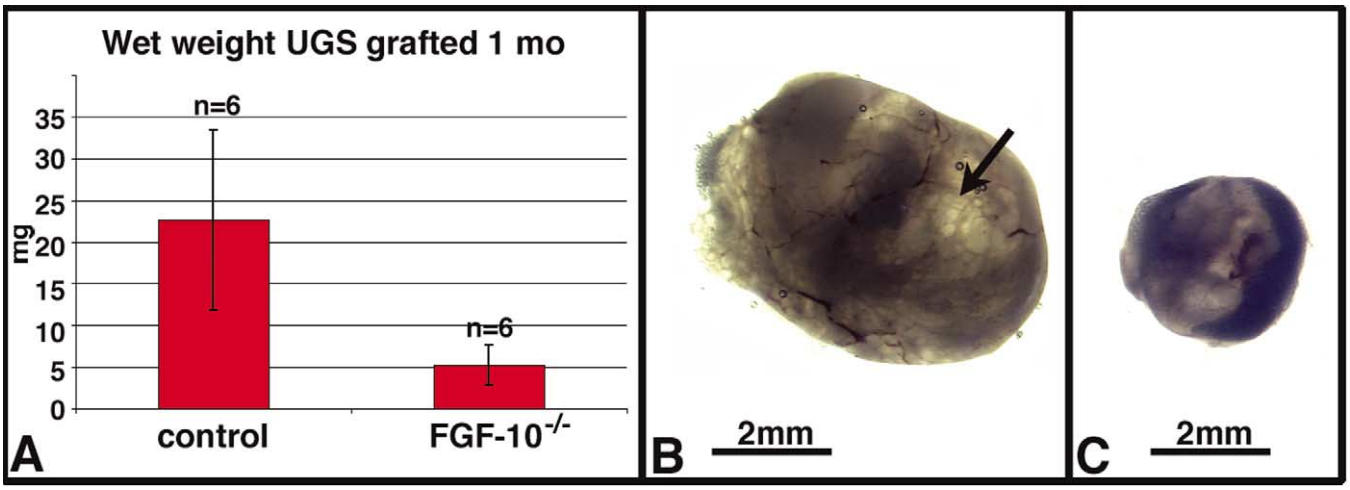

Fig. 5. Grafted FGF-$10^{-/-}$ UGS are smaller and less ductal than controls. (A) The mean wet weight (±95% confidence intervals) of control vs. FGF-$10^{-/-}$ UGS, aged 15-19 dpc, grafted into intact, nude male mouse hosts for 1 month. FGF-$10^{-/-}$ UGSs were significantly smaller than controls ($P < 0.05$). (B) Whole-mount image of a control UGS grafted for 1 month, 18 dpc at the start. The ductal structure of the graft can be seen (arrow). (C) Whole-mount image of a FGF-$10^{-/-}$ UGS, 18 dpc at the start, grafted for 1 month. No ductal structure was apparent.

of eight grafted WD developed into SV. The seminal vesicle mesenchyme expresses high levels of FGF-10 (Thomson and Cunha, 1999), so the seminal vesicle might be expected to also show an organ-specific defect in the absence of FGF-10. It is not known whether the caudal WD mesenchyme expresses FGF-10. In the caudal WD, as in the seminal vesicle, testosterone appears to act indirectly via the mesenchyme (Drews, 2000), and thus a paracrine role for FGF-10 is possible.

The primary reason for prostatic agenesis in FGF-$10^{-/-}$ mice appears to be the absence of FGF-10 rather than suboptimal testosterone. While UGSs of all embryonic ages from both male and female control mice develop into mature prostate when grown for 1 month in intact, adult male nude mouse hosts (Cunha, 1975; Cunha et al., 1980), UGSs from FGF-$10^{-/-}$ fetuses did not develop into prostate under these circumstances. This indicates that supplying adult levels of testosterone cannot reverse the FGF-$10^{-/-}$ phenotype. Thus, FGF-10 is required for prostatic development. Prostatic development was partially restored when the FGF-$10^{-/-}$ UGSs were cultured with testosterone plus FGF-10. The partial nature of this restoration may be due to an inadequate concentration of FGF-10 in the medium, or that 4 days may not be enough time for the FGF-$10^{-/-}$ UGS to "catch up." Female UGS in culture require more time in the presence of testosterone than male UGS to generate buds (Takeda et al., 1986). When UGSs from older (19.5 dpc) female rat fetuses are cultured in the presence of androgens, they generate fewer prostatic buds than do younger UGSs or male UGSs (Lasnitzki and Mizuno, 1977). In this study, age-matched UGSs were cultured simultaneously with FGF-$10^{-/-}$ to reduce UGS age as a confounding factor. In addition, FGF-10 was present in the control UGS but not in the FGF-$10^{-/-}$ UGS prior to culture, which may suggest that FGF10 plays an early role in patterning prostatic budding from the UGS.

Is FGF-10 a prostatic inducer? Clearly, FGF-10 is necessary for growth and branching morphogenesis of the prostate gland. However, FGF-10 meets only two of the three criteria for an inductive signal (Slack, 1993). The first criterion that FGF-10 fulfills is that it is present at the time of the induction of prostatic buds and is expressed in the mesenchyme that is known to send the inductive signal. Secondly, the absence of an inductive signal must result in the absence of the organ. This was true in the FGF-$10^{-/-}$ mice. The final criterion for an inductive signal, which is not fulfilled by FGF-10 in the prostate, is that the molecule should be sufficient to induce organ development. FGF-10 was unable to stimulate prostatic budding in urogenital sinuses in the absence of testosterone. Although FGF-10 does not meet these criteria for an instructive inductor, our data suggest that it plays a key permissive role in early event during the induction of the prostate.

The histological appearance of the FGF-$10^{-/-}$ urogenital sinuses is potentially informative with regards to the very early events of prostatic induction. These early events have been generally referred to as "bud induction." In some developing structures, such as the feather, budding events are preceded by a placode stage that follows biochemical commitment but precedes feather budding (Séngel, 1976). In the prostate, no comparable thickening of the epithelium, or placode stage has been identified. However the structures formed by indentations of the basal lamina (Figs. 6 and 9) may represent a kind of prebud stage similar to that seen in the lung (Miura and Shiota, 2000; Nogawa et al., 1998). The first event in the morphogenesis of lung epithelium is a slight clefting of the basal lamina at irregular intervals (Miura and Shiota, 2000; Nogawa et al., 1998). This pre-

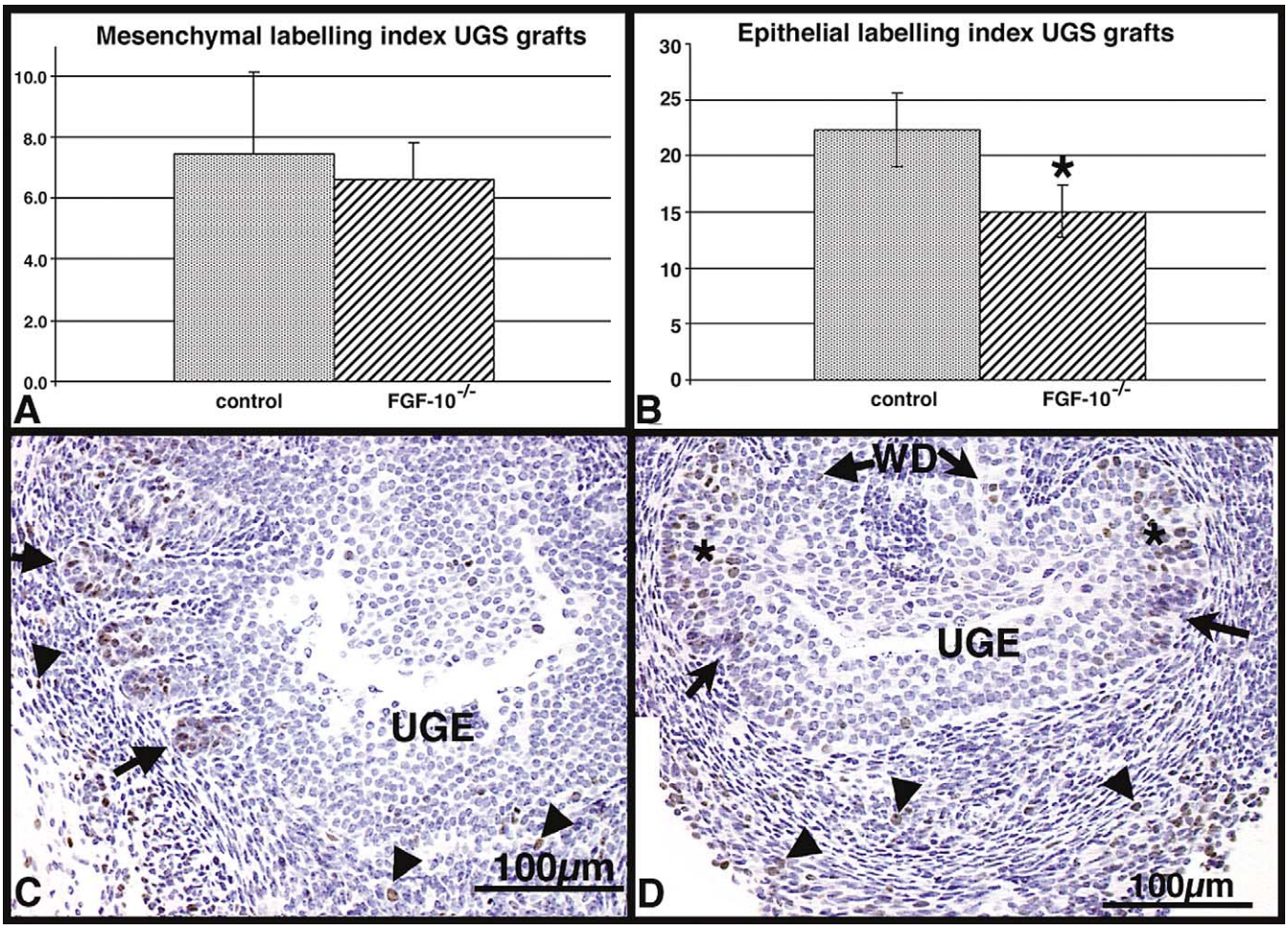

Fig. 6. Proliferation in FGF-$10^{-/-}$ and control tissues. (A) Mesenchymal labeling index was not statistically different in control and FGF-$10^{-/-}$ UGSs grafted for 2 weeks ($n = 3$/per group, mean ± 95% C.I.). (B) Epithelial labeling index was greater (*, $P < 0.05$) in control than in FGF-$10^{-/-}$ UGS grafted for 2 weeks ($n = 10$ per group, mean ± 95% C.I.). (C) In the control UGS (18.5 dpc), the prostatic ducts were heavily labeled by an antibody against Ki67, indicating a high rate of proliferation (arrows) as compared with the UGE from which they budded. Mesenchymal cells were also proliferating (arrowheads). (D) In UGS from FGF-$10^{-/-}$ fetuses (18.5 dpc), prostatic ducts are not present, but indentations of the basal lamina (arrows) border areas of the UGE that appear to have more Ki67-labeled cells (*). Mesenchymal labeling was similar to the control (arrowheads). The Wolffian ducts (WD) can be seen joining the UGS at the top (dorsal) of the panel.

cedes differential proliferation (Nogawa et al., 1998). Bud induction may therefore be thought of as a two-step process, the first step being the formation of clefts and irregular buds and the second step being the stabilization and outgrowth of these transient buds (Fig. 9).

Time-lapse photography of cultured neonatal bulbourethral gland (Cunha unpublished observation) suggests that the early phase of bud formation is also a dynamic process, with many small incipient buds forming and disappearing. Only some of these transient buds become stabilized and continue to grow and contribute to the adult gland. If this is true in the male UGS, and if FGF-10 is the stabilizing/growth factor for nascent buds, histological sections of FGF-$10^{-/-}$ UGS would represent a snapshot of an organ rudiment stuck in that first step of transient bud formation, which may explain the relative paucity of final buds in the FGF-$10^{-/-}$ UGS (Fig. 9). It is possible that the UGE contains a constitutive pathway for epithelial budding which is

Fig. 7. Organ culture (4 days) of control and FGF-$10^{-/-}$ UGS. (A) A control UGS, 15.5 dpc at the start, grown in the presence of testosterone (10^{-8} M) developed prostatic ducts and occasional clefts (arrow). (B) An FGF-$10^{-/-}$ UGS, 16.5 dpc at the start, grown in the presence of testosterone did not develop prostatic ducts (same scale as in A). (C) A control UGS, 15.5 dpc at the start, grown in the presence of 200 ng/ml of FGF-10, but no testosterone, did not develop prostatic ducts (same scale as in A). (D) Explant growth in organ culture (percent increase in area mean ± 95% confidence intervals) of control UGS grown in the presence or absence of testosterone and/or FGF-10. All groups with the same letter designation are statistically the same, while groups with different letters (three groups, a–c) are statistically different from each other ($P < 0.05$). (E) A control UGS, 15.5 dpc at the start, grown in the presence of testosterone and FGF-10. Note the wideness of the ducts and several branch points (arrows, same scale as in A). (F) An FGF-$10^{-/-}$ UGS, 15.5 dpc at the start, grown in the presence of testosterone (10^{-8} M) and FGF-10 (200 ng/ml). Prostatic buds formed (arrows).

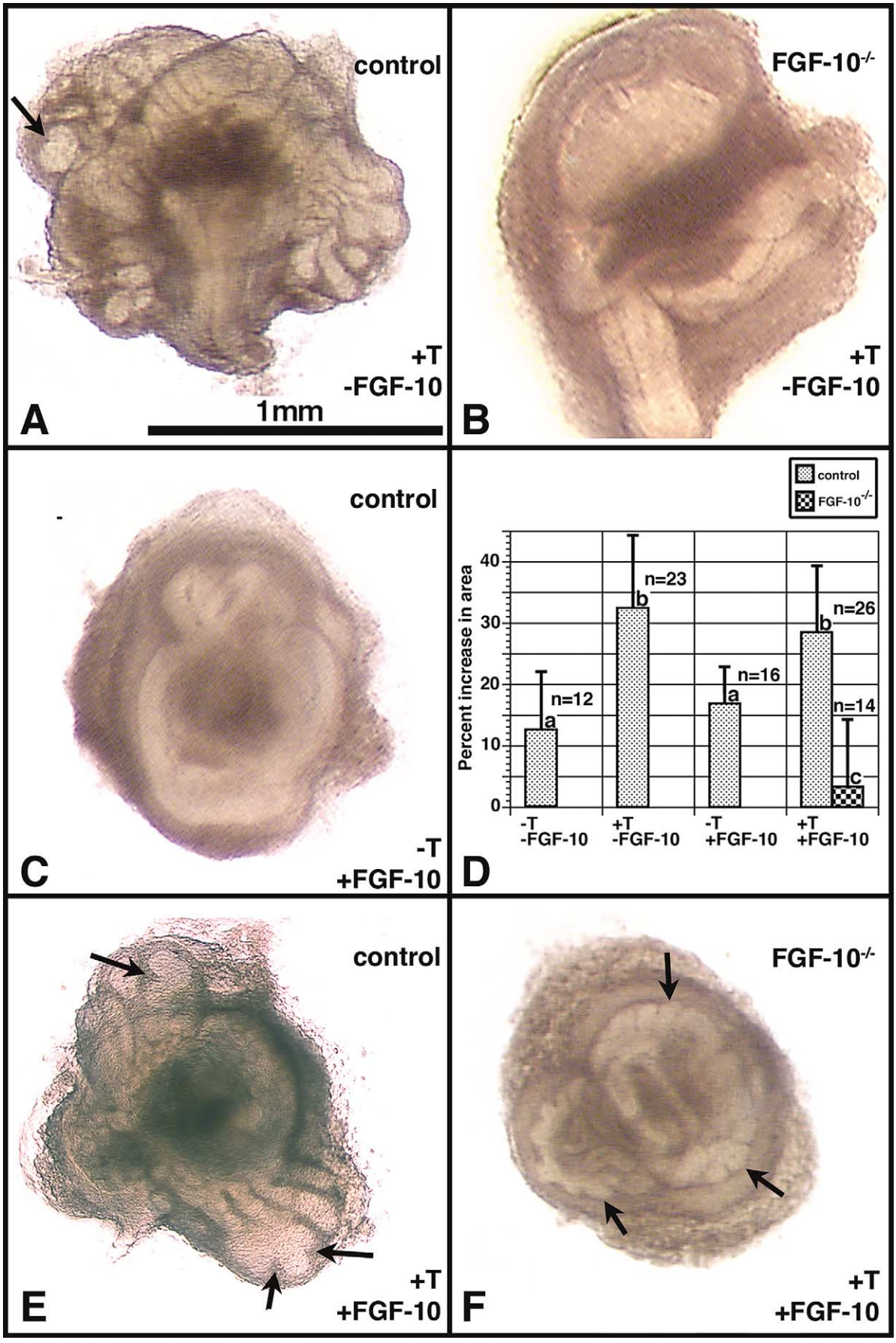
control
+T
-FGF-10
1mm
A
FGF-10-/-
+T
-FGF-10
B
control
-T
+FGF-10
C
control
FGF-10-/-
Percent increase in area
40
30
20
10
0
n=12
a
n=23
b
n=16
a
n=26
b
n=14
c
-T
-FGF-10
+T
-FGF-10
-T
+FGF-10
+T
+FGF-10
D
control
+T
+FGF-10
E
FGF-10-/-
+T
+FGF-10
F

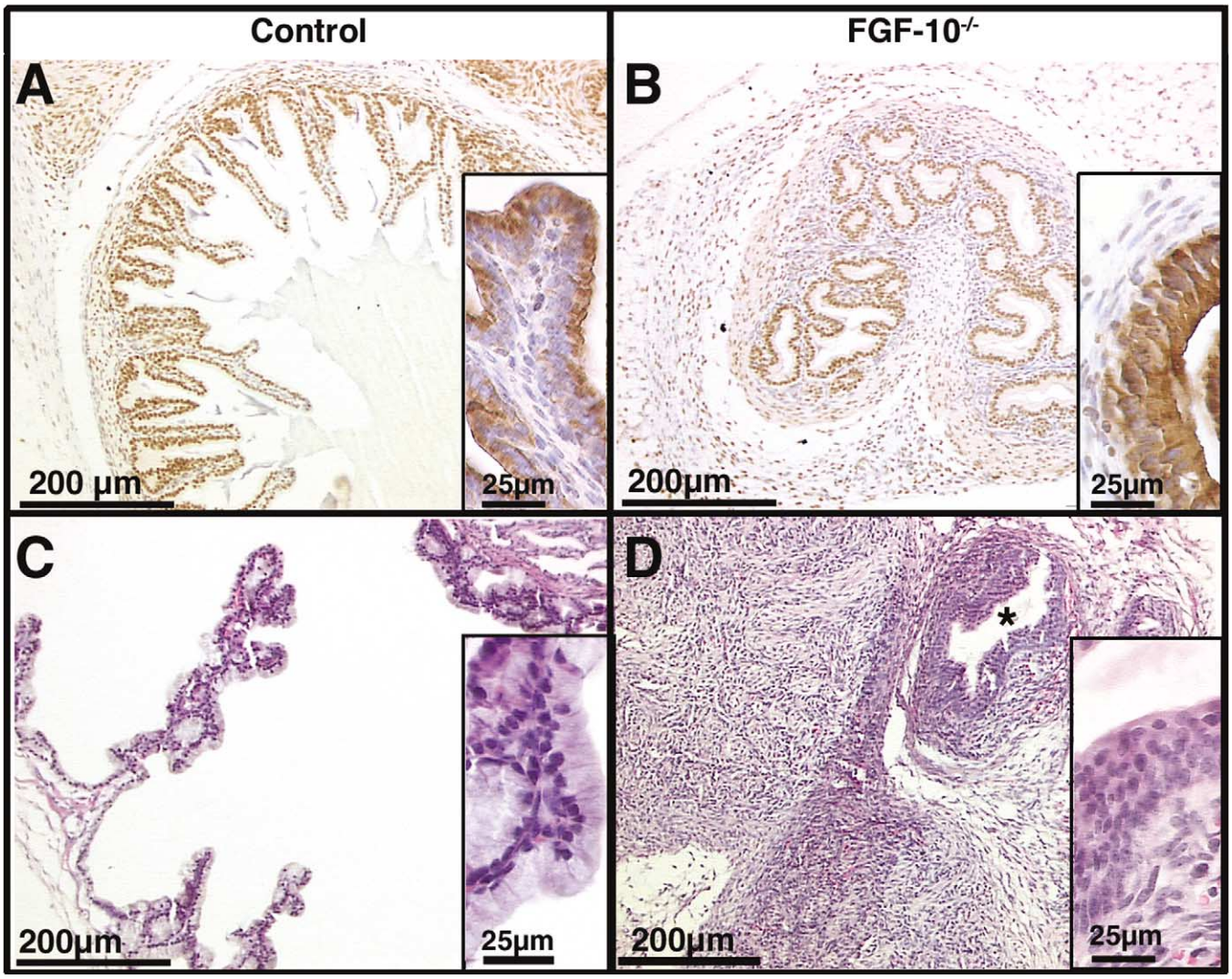

Fig. 8. Histology of grafts of the lower Wölffian ducts (A, B) and lower urethra (C, D) from control (A, C) and FGF-$10^{-/-}$ fetuses. (A) Control grafts showed typical adult SV histology with papillary folds. Anti-androgen receptor immunocytochemistry showed strong staining of the tall columnar epithelial cells. Staining with anti-mouse SV proteins (inset). (B) This FGF-$10^{-/-}$ graft showed histology typical of the immature SV, which had more stroma, lower columnar epithelium and a smaller lumen than controls. The low columnar cells showed strong staining with anti-androgen receptor antibody (brown). Staining with anti-mouse SV proteins (inset). (C) Grafts of the control lower urethra developed into bulbourethral gland. The epithelial cells were filled with mucous (inset). Hematoxylin and eosin stain. (D) Grafts of the FGF-$10^{-/-}$ lower urethra were mostly composed of dense stroma; the epithelium was stratified and resembled urothelium (* and inset). Hematoxylin and eosin stain.

independent of androgen action. This may explain the observation of prostate-like buds in female rat embryos, though prostatic buds in females are observed at low frequency (Timms et al., 1999)

In grafted FGF-$10^{-/-}$ UGS, clefts and early buds formed. Under the influence of continuous adult levels of testosterone, epithelial cells of these rudimentary structures expressed androgen receptors and eventually responded to a differentiation cue, which may be testosterone itself, and produced prostatic secretory proteins, albeit at low levels. Therefore, the first step in prostatic development, commitment and transient bud formation, and the last step, secretory cytodifferentiation, appear to occur in the absence of FGF-10 and the cellular processes that it controls (Fig. 9).

The role of FGF-10 in the growth of established prostatic ducts has been clearly demonstrated in cultures of neonatal rat ventral prostate (VP) in which FGF-10 (and FGF-7) are able to support branching morphogenesis in the absence of testosterone (Sugimura et al., 1996; Thomson and Cunha, 1999). In these rat VP organ cultures, the original budding events had occurred prior to culture and initial dichotomous branching was already underway. This stimulation of continued ductal growth and branching is essential to the growth of a normal prostate, but occurs several days after prostatic bud induction. Bud induction and stimulation of ductal growth are different events and may be under the control of different molecules.

Testosterone qualifies as an inductive signal for the pros-

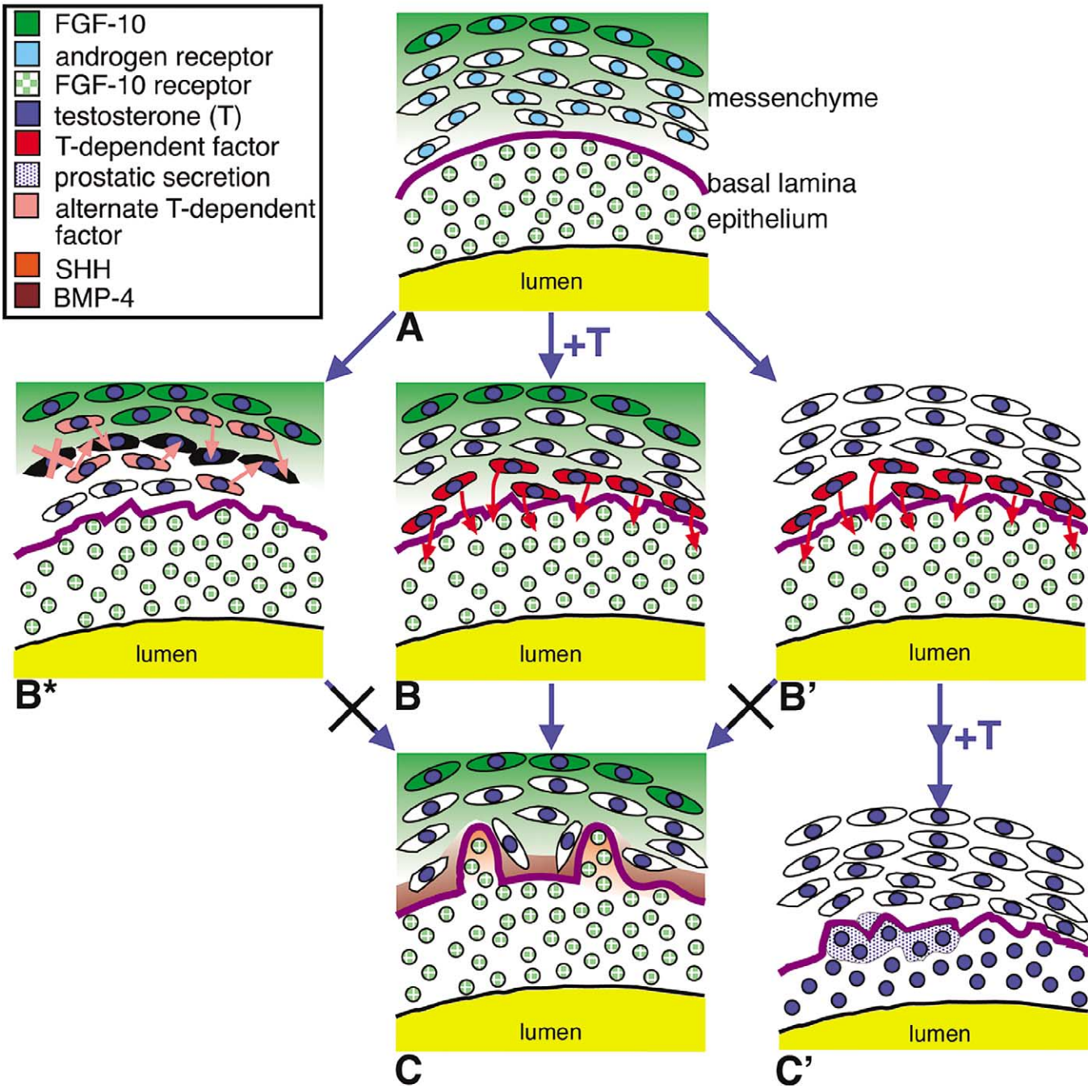

Fig. 9. Diagram of a model for regulation of the early events in prostatic budding. (A) The UGS prior to testosterone secretion or the female UGS. FGF-10 is produced by mesenchymal cells some distance from the epithelium and presumably has some ability to diffuse toward the epithelium. Mesenchymal cells, and not epithelial cells, have androgen receptors; FGF-10 production is not dependent on androgens. Epithelial cells, but not mesenchymal cells, have receptors for FGF-10 (FGFR2IIIb). (B) The proposed prebud or transient bud stage in a normal male. Testosterone acts on the mesenchyme to stimulate production of an unknown factor. This factor acts on the epithelium or the extracellular matrix/basal lamina to promote epithelial clefting and/or transient budding. Close to the epithelium FGF-10 does not reach an effective threshold level. (B*) An alternative pathway for androgen action. The black cells represent a barrier to FGF-10 action. This barrier could be a band of smooth muscle. The function of the unknown, androgen-dependent factor could be to prevent barrier formation, or to break down a barrier either by acting on the barrier cells or on adjacent cells so that FGF-10 can reach the epithelium at above threshold levels. (B′) The UGS in FGF-$10^{-/-}$ males. The unknown mesenchymal factor is produced in response to testosterone and acts on the epithelium, but buds cannot be stabilized nor promoted and therefore remain in the prebud stage because these latter events are FGF-10-dependent. (C) The stabilized/growing bud phase. Some buds have reached into the area of mesenchyme where FGF-10 is above the threshold. Therefore, the buds increase their growth rate and do not collapse back into the UGE. Shh is expressed in the epithelium, and BMP-4 is expressed in the mesenchyme (Lamm et al., 2002). (C′) The UGS in FGF-$10^{-/-}$ males grafted for 1 month in an intact male host. Some clefting remains, but there is no ductal growth. The epithelial cells now express androgen receptors and produce prostatic secretory proteins.

tate, as it is necessary and sufficient for prostatic development and is present at the correct time. As an endocrine factor, the inductive actions of testosterone and/or its metabolites extend beyond the prostate to all of the secondary sex organs. The influence of androgens on the epithelium is indirect (Cunha et al., 1987) acting via signals, "downstream inducers" produced by the mesenchyme. FGF-10 is clearly a mesenchymal signal required for prostatic development and growth, but it is not the only one. In addition, FGF-10 is not directly regulated by testosterone, at least in the neonatal prostate and SV (Thomson and Cunha, 1999). Any signal for instructive induction of the prostate must be directly or indirectly androgen-dependent. It is possible that FGF10 protein diffusion is regulated by an androgen-sensitive layer of smooth muscle which forms between inductive UGM and UGE (Fig. 9) (Thomson et al., 2002).

FGF-10 clearly affects epithelial proliferation in the developing prostate. Urogenital sinus epithelium from both control and FGF-$10^{-/-}$ mice had significantly lower labeling indices than the prostatic buds emerging from the UGE. In grafts, epithelial labeling index was significantly less in FGF-$10^{-/-}$ than in control tissue. In the lung and pancreas, FGF-10 stimulates epithelial proliferation (Bhushan et al., 2001; Park et al., 1998). Elongating prostatic buds grow toward the source of FGF-10, the mesenchymal cells, which lie peripherally in specialized zones with in the UGM (Thomson and Cunha, 1999). In rat the FGF-10-producing cells reside in the ventral mesenchymal pad, which is readily identifiable in hematoxylin and eosin-stained sections (Timms et al., 1995). Apoptosis was not affected by FGF-10. Programmed cell death was uniformly low in both control and FGF-$10^{-/-}$ UGSs and prostatic grafts examined. FGF-10 has been shown to stimulate cell migration in the lung (Park et al., 1998). This remains a possibility in the prostate.

FGF-10 appears to be an essential factor in branching morphogenesis in several organs; however, its location in the hierarchy of signals varies. FGF-10 acts as a true inductive signal for both the lacrimal and Harderian glands where it is both necessary and sufficient for gland induction and development (Govindarajan et al., 2000). In both the pancreas (Bhushan et al., 2001) and lung (Min et al., 1998), the initial epithelial outgrowths form in the absence of FGF-10 but then do not proliferate or branch. The prostate appeared to use FGF-10 in a way that was more similar to the lung and pancreas than the Harderian and lacrimal glands.

FGF-10 is likely to interact with other growth factors involved in branching morphogenesis as it does in other organs. Bone morphogenetic proteins (BMPs) are members of the transforming growth factor superfamily (Wozney et al., 1988). BMP-4, as demonstrated by immunocytochemistry, is localized close to the early prostatic buds in the UGS (Lamm et al., 2001), while FGF-10 producing mesenchymal cells are separated from the epithelium by a gap of FGF-10 nonexpressing cells (Fig. 9). As branching morphogenesis proceeds, BMP-4 becomes concentrated at branch-points and FGF-10 at ductal tips. These two growth factors have opposite effects on branching morphogenesis; FGF-10 stimulates ductal growth, while BMP-4 inhibits it. Neither of these two molecules is androgen-dependent. In the lung and tooth, FGF-10 and BMP-4 antagonize each other's actions and may interact to establish tooth and lung bud spacing (Weaver et al., 2000). This may occur also in the prostate, once branching morphogenesis is initiated.

Sonic hedgehog (Shh) is produced by prostatic buds and urogenital sinus epithelium (Lamm et al., 2002; Podlasek et al., 1999). Blocking antibodies to Shh inhibit prostatic development (Podlasek et al., 1999). Podlasek et al. have reported that *Shh* transcript expression was increased in UGS in response to androgens, concluding that androgen-induced expression of *Shh* in the UGS is necessary for prostatic induction. However, in the UGM, the expression of BMP4, a putative downstream signaling effector of the Shh-signaling pathway (Bitgood and McMahon, 1995), is not dependent on androgens (Lamm et al., 2001). In the lung, Shh stimulates mesenchymal proliferation and decreases levels of FGF-10 (Bellusci et al., 1997a,b). Sonic hedgehog is present in the UGE at the time of initial prostatic bud formation and could be involved in this process; however, it is unlikely to be regulated directly by testosterone as prostatic budding can occur in the absence of epithelial androgen receptors (Cunha and Chung, 1981; Cunha and Lung, 1978; Shannon and Cunha, 1984). Thus, an androgen-dependent mesenchymal factor that initiates budding remains to be identified. Future approaches are likely to include microarray searches for novel factors as well as examining the roles of known growth factors.

Acknowledgments

We thank Dr. Scott Simonet from Amgen Inc. for generously providing the breeding pairs of FGF-$10^{+/-}$ mice and Dr. Stephen Higgins for providing the antibody to mouse seminal vesicle secretion. This work was supported by the National Institutes Grants DK 47517, DK 52708, CA64872, CA 59831, CA 84294, and CA89520. Dr. Thomson is supported by the MRC and CDMRP Prostate Cancer Research Program DAMD17-00-1-0034.

References

Bellusci, S., Furuta, Y., Rush, M.G., Henderson, R., Winnier, G., Hogan, B.L., 1997a. Involvement of Sonic hedgehog (Shh) in mouse embryonic lung growth and morphogenesis. Development 124, 53–63.

Bellusci, S., Grindley, J., Emoto, H., Itoh, N., Hogan, B.L.M., 1997b. Fibroblast Growth Factor 10(FGF10) and branching morphogenesis in the embryonic mouse lung. Development 124, 4867–4878.

Bhushan, A., Itoh, N., Kato, S., Thiery, J.P., Czernichow, P., Bellusci, S., Scharfmann, R., 2001. Fgf10 is essential for maintaining the proliferative capacity of epithelial progenitor cells during early pancreatic organogenesis. Development 128, 5109–5117.

Bitgood, M.J., McMahon, A.P., 1995. Hedgehog and Bmp genes are coexpressed at many diverse sites of cell–cell interaction in the mouse embryo. Dev. Biol. 172, 126–138.

Cunha, G.R., 1975. Age-dependent loss of sensitivity of female urogenital sinus to androgenic conditions as a function of the epithelial–stromal interaction. Endocrinology 95, 665–673.

Cunha, G.R., Chung, L.W.K., 1981. Stromal-epithelial interactions: I. Induction of prostatic phenotype in urothelium of testicular feminized (Tfm/y) mice. J. Steroid Biochem. 14, 1317–1321.

Cunha, G.R., Chung, L.W.K., Shannon, J.M., Reese, B.A., 1980. Stromal–epithelial interactions in sex differentiation. Biol. Reprod. 22, 19–43.

Cunha, G.R., Donjacour, A.A., 1987. Mesenchymal-epithelial interactions: technical considerations, in: Coffey, D.S., Bruchovsky, N., Gardner, W.A., Resnick, M.I., Karr, J.P. (Eds.), Assessment of Current Concepts and Approaches to the Study of Prostate Cancer, A.R. Liss, New York, pp. 273–282.

Cunha, G.R., Donjacour, A.A., Cooke, P.S., Mee, S., Bigsby, R.M., Higgins, S.J., Sugimura, Y., 1987. The endocrinology and developmental biology of the prostate. Endocr. Rev. 8, 338–362.

Cunha, G.R., Fujii, H., Neubauer, B.L., Shannon, J.M., Sawyer, L.M., Reese, B.A., 1983. Epithelial–mesenchymal interactions in prostatic development. I. Morphological observations of prostatic induction by urogenital sinus mesenchyme in epithelium of the adult rodent urinary bladder. J. Cell Biol. 96, 1662–1670.

Cunha, G.R., Lung, B., 1978. The possible influences of temporal factors in androgenic responsiveness of urogenital tissue recombinants from wild-type and androgen-insensitive (Tfm) mice. J. Exp. Zool. 205, 181–194.

Donjacour, A.A., Rosales, A., Higgins, S.J., Cunha, G.R., 1990. Characterization of antibodies to androgen-dependent secretory proteins of the mouse dorsolateral prostate. Endocrinology 126, 1343–1354.

Drews, U., 2000. Local mechanisms in sex specific morphogenesis. Cytogenet. Cell. Genet. 91, 72–80.

Finch, P.W., Cunha, G.R., Rubin, J.S., Wong, J., Ron, D., 1995. Pattern of KGF and KGFR expression during mouse fetal development suggests a role in mediating morphogenetic mesenchymal–epithelial interactions. Dev. Dyn. 203, 223–240.

Foster, B.A., Kaplan, P.J., Greenberg, N.M., 1999. Changes in the expression of FGF-7, FGF-10 and a novel FGFR1iiic splice form correlate with prostate cancer progression in the TRAMP model. Prostate Cancer and Prostatic Diseases 2, 76–82.

Gallee, M.P., Visser-de Jong, E., ten Kate, F.J., Schroeder, F.H., Van der Kwast, T.H., 1989. Monoclonal antibody Ki-67 defined growth fraction in benign prostatic hyperplasia and prostatic cancer. J. Urol. 142, 1342–1346.

Govindarajan, V., Ito, M., Makarenkova, H.P., Lang, R.A., Overbeek, P.A., 2000. Endogenous and ectopic gland induction by FGF-10. Dev. Biol. 225, 188–200.

Guo, L., Degenstein, L., Fuchs, E., 1996. Keratinocyte growth factor is required for hair development but not for wound healing. Genes Dev. 10, 165–175.

Higgins, S.J., Young, P., Brody, J.R., Cunha, G.R., 1989. Induction of functional cytodifferentiation in the epithelium of tissue recombinants. I. Homotypic seminal vesicle recombinants. Development 106, 219–234.

Hogan, B.L., 1999. Morphogenesis. Cell 96, 225–233.

Jones, E.C., Krohn, P.L., 1960. Orthotopic ovarian transplantation in mice. J. Endocrinol. 20, 135–145.

Jost, A., 1971. Embryonic sexual differentiation (Morphology, Physiology, Abnormalities), in: Jones, H.W., Scott, W.W. (Eds.), Hermaphroditism, Genital Anomalies and Related Endocrine Disorders, Williams and Wilkins, Baltimore, pp. 15–45.

Kurita, T., Wang, Y.Z., Donjacour, A.A., Zhao, C., Lydon, J.P., O'Malley, B.W., Isaacs, J.T., Dahiya, R., Cunha, G.R., 2001. Paracrine regulation of apoptosis by steroid hormones in the male and female reproductive system. Cell Death Differ. 8, 192–200.

Lamm, M.L., Podlasek, C.A., Barnett, D.H., Lee, J., Clemens, J.Q., Hebner, C.M., Bushman, W., 2001. Mesenchymal factor bone morphogenetic protein 4 restricts ductal budding and branching morphogenesis in the developing prostate. Dev. Biol. 232, 301–314.

Lamm, M.L.G., Catbagan, W.S., Laciak, R.J., Barnett, D.H., Hebner, C.M., Gaffield, W., Walterhouse, D., Iannaccone, P., Bushman, W., 2002. Sonic hedgehog activates mesenchymal *Gli1* expression during prostate ductal bud formation. Dev. Biol. 249, 349–366.

Lasnitzki, I., Mizuno, T., 1977. Induction of the rat prostate gland by androgens in organ culture. J. Endocrinol. 74, 47–55.

Lu, W., Luo, Y., Kan, M., McKeehan, W.L., 1999. Fibroblast growth factor-10. A second candidate stromal to epithelial cell andromedin in prostate. J. Biol. Chem. 274, 12827–12834.

Martin, G., 2001. Making a vertebrate limb: new players enter from the wings. Bioessays 23, 865–868.

Mason, I.J., Pace, F.F., Smith, R., Dickson, C., 1994. FGF-7 (keratinocyte growth factor) expression during mouse development suggests roles in myogenesis, forebrain regionalization and epithelial–mesenchymal interactions. Mech. Dev. 15, 15–30.

McKeehan, W.L., Wang, F., Kan, M., 1998. The heparan sulfate-fibroblast growth factor family: diversity of structure and function. Prog. Nucleic Acid Res. Mol. Biol. 59, 135–176.

Min, H., Danilenko, D., Scully, S., Bolon, B., Ring, B., Tarpley, J., DeRose, M., Simonet, W., 1998. Fgf-10 is required both limb and lung development and exhibits striking functional similarity to Drosophila branchless. Genes Dev. 20, 3156–3161.

Miura, T., Shiota, K., 2000. Time-lapse observation of branching morphogenesis of the lung bud epithelium in mesenchyme-free culture and its relationship with the localization of actin filaments. Int. J. Dev. Biol. 44, 899–902.

Nogawa, H., Morita, K., Cardoso, W.V., 1998. Bud formation precedes the appearance of differential cell proliferation during branching morphogenesis of mouse lung epithelium in vitro. Dev. Dyn. 213, 228–235.

O'Shaughnessy, P.J., Baker, P., Sohnius, U., Haavisto, A.M., Charlton, H.M., Huhtaniemi, I., 1998. Fetal development of Leydig cell activity in the mouse is independent of pituitary gonadotroph function. Endocrinology 139, 1141–1146.

Ohuchi, H., Hori, Y., Yamasaki, M., Harada, H., Sekine, K., Kato, S., Itoh, N., 2000. FGF10 acts as a major ligand for FGF receptor 2 IIIb in mouse multi- organ development. Biochem. Biophys. Res. Commun. 277, 643–649.

Orr-Urtreger, A., Bedford, M.T., Burakova, T., Arman, E., Zimmer, Y., Yayon, A., Givol, D., Lonai, P., 1993. Developmental localization of the splicing alternatives of fibroblast growth factor receptor-2 (FGFR2). Dev. Biol. 158, 475–486.

Park, W.Y., Miranda, B., Lebeche, D., Hashimoto, G., Cardoso, W.V., 1998. FGF-10 is a chemotactic factor for distal epithelial buds during lung development. Dev. Biol. 201, 125–134.

Peters, K., Werner, S., Liao, X., Wert, S., Whitsett, J., Williams, L., 1994. Targeted expression of a dominant negative FGF receptor blocks branching morphogenesis and epithelial differentiation of the mouse lung. EMBO J. 12, 973–986.

Podlasek, C.A., Barnett, D.H., Clemens, J.Q., Bak, P.M., Bushman, W., 1999. Prostate development requires Sonic hedgehog expressed by the urogenital sinus epithelium. Dev. Biol. 209, 28–39.

Sekine, K., Ohuchi, H., Fujiwara, M., Yamasaki, M., Yoshizawa, T., Sato, T., Yagishita, N., Matsui, D., Koga, Y., Itoh, N., Kato, S., 1999. Fgf10 is essential for limb and lung formation. Nat. Genet. 21, 138–141.

Séngel, P., 1976. Morphogenesis of Skin. Cambridge University Press, Cambridge.

Shannon, J.M., Cunha, G.R., 1984. Characterization of androgen binding and deoxyribonucleic acid synthesis in prostate-like structures induced in testicular feminized (Tfm/Y) mice. Biol. Reprod. 31, 175–183.

Signoretti, S., Waltregny, D., Dilks, J., Isaac, B., Lin, D., Garraway, L., Yang, A., Montironi, R., McKeon, F., Loda, M., 2000. p63 is a prostate basal cell marker and is required for prostate development. Am. J. Pathol. 157, 1769–1775.

Simonet, W.S., DeRose, M.L., Bucay, N., Nguyen, H.Q., Wert, S.E., Zhou, L., Ulich, T.R., Thomason, A., Danilenko, D.M., Whitsett, J.A., 1995. Pulmonary malformation in transgenic mice expressing human keratinocyte growth factor in the lung. Proc. Natl. Acad. Sci. USA 92, 12461–12465.

Slack, J.M., 1993. Embryonic induction. Mech. Dev. 41, 91–107.

Sugimura, Y., Foster, B.A., Hom, Y.K., Rubin, J.S., Finch, P.W., Aaronson, S.A., Hayashi, N., Kawamura, J., Cunha, G.R., 1996. Keratinocyte growth factor (KGF) can replace testosterone in the ductal branching morphogenesis of the rat ventral prostate. Int. J. Dev. Biol. 40, 941–951.

Sutherland, D., Samakovlis, C., Krasnow, M.A., 1996. Branchless encodes a Drosophila FGF homolog that controls tracheal cell migration and the pattern of branching. Cell 87, 1091–1101.

Suzuki, K., Yamanishi, K., Mori, O., Kamikawa, M., Andersen, B., Kato, S., Toyoda, T., Yamada, G., 2000. Defective terminal differentiation and hypoplasia of the epidermis in mice lacking the Fgf10 gene. FEBS Lett. 481, 53–56.

Szebenyi, G., Fallon, J.F., 1999. Fibroblast growth factors as multifunctional signaling factors. Int. Rev. Cytol. 185, 45–106.

Takeda, H., Lasnitzki, I., and Mizuno, T., 1986. Analysis of prostatic bud induction by brief androgen treatment in the fetal rat urogenital sinus. J. Endocrinology 110, 467–470.

Thomson, A.A., 2001. Role of androgens and fibroblast growth factors in prostatic development. Reproduction 121, 187–195.

Thomson, A.A., Cunha, G.R., 1999. Prostatic growth and development are regulated by FGF10. Development 126, 3693–3701.

Thomson, A.A., Foster, B.A., Cunha, G.R., 1997. Analysis of growth factor and receptor mRNAs during development of the rat seminal vesicle and prostate. Development 124, 2431–2439.

Thomson, A.A., Timms, B.G., Barton, L., Cunha, G.R., Grace, O.C., 2002. The role of smooth muscle in regulating prostatic induction. Development 129, 1905–1912.

Timms, B., Lee, C., Aumuller, G., Seitz, J., 1995. Instructive induction of prostate growth and differentiation by a defined urogenital sinus mesenchyme. Microsc. Res. Tech. 30, 319–332.

Timms, B.G, Ptersen, S.L., vom Saal, F. S., 1999. Prostate gland growth during development is stimulated in both male and female rat fetuses by intrauterine proximity to female fetuses. J. Urol. 161, 1694–1701.

Weaver, M., Dunn, N.R., Hogan, B.L., 2000. Bmp4 and Fgf10 play opposing roles during lung bud morphogenesis. Development 127, 2695–2704.

Wozney, J.M., Rosen, V., Celeste, A.J., Mitsock, L.M., Whitters, M.J., Kriz, R.W., Hewick, R.M., Wang, E.A., 1988. Novel regulators of bone formation: molecular clones and activities. Science 242, 1528–1534.